Am J Physiol Gastrointest Liver Physiol 294: G27–G38, 2008.
First published October 18, 2007; doi:10.1152/ajpgi.00296.2007.

A new model for nonalcoholic steatohepatitis in the rat utilizing total enteral nutrition to overfeed a high-polyunsaturated fat diet

January N. Baumgardner,[1,4] Kartik Shankar,[1,4] Leah Hennings,[3] Thomas M. Badger,[1,2,4] and Martin J. J. Ronis[1,4]

[1]*Departments of Pharmacology and Toxicology,* [2]*Physiology and Biophysics and* [3]*Pathology, University of Arkansas for Medical Sciences; and* [4]*Arkansas Children's Nutrition Center, Little Rock, Arkansas*

Submitted 28 June 2007; accepted in final form 15 October 2007

Baumgardner JN, Shankar K, Hennings L, Badger TM, Ronis MJ. A new model for nonalcoholic steatohepatitis in the rat utilizing total enteral nutrition to overfeed a high-polyunsaturated fat diet. *Am J Physiol Gastrointest Liver Physiol* 294: G27–G38, 2008. First published October 18, 2007; doi:10.1152/ajpgi.00296.2007.—We have used total enteral nutrition (TEN) to moderately overfeed rats high-polyunsaturated fat diets to develop a model for nonalcoholic steatohepatitis (NASH). Male Sprague-Dawley rats were fed by TEN a 187 kcal·kg$^{-3/4}$·day^{-1} diet containing 5% (total calories) corn oil or a 220 kcal·kg$^{-3/4}$·day^{-1} diet in which corn oil constituted 5, 10, 25, 35, 40, or 70% of total calories for 21 or 65 days. Rats fed the 5% corn oil, 220 kcal·kg$^{-3/4}$·day^{-1} diet had greater body weight gain ($P \leq 0.05$), fat mass ($P \leq 0.05$), and serum leptin and glucose levels ($P \leq 0.05$), but no liver pathology. A dose-dependent increase in hepatic triglyceride deposition occurred with increase in percent corn oil in the 220 kcal·kg$^{-3/4}$·day^{-1} groups ($P \leq 0.05$). Steatosis, macrophage infiltration, apoptosis, and focal necrosis were present in the 70% corn oil group, accompanied by elevated serum alanine aminotransferase (ALT) levels ($P \leq 0.05$). An increase in oxidative stress (thiobarbituric acid-reactive substances) and TNF-α expression ($P \leq 0.05$) was observed in the 70% corn oil group, as well as an increase in hepatic CYP2E1 and CYP4A1 expression ($P \leq 0.05$). Significant positive correlations were observed between the level of dietary corn oil and the degree of pathology, ALTs, oxidative stress, and inflammation. Liver pathology was progressive with increased necrosis, accompanied by fibrosis, observed after 65 days of TEN. Increased expression of CD36 and L-FABP mRNA suggested development of steatosis was associated with increased fatty acid transport. These data suggest that intragastric infusion of a high-polyunsaturated fat diet at a caloric level of 17% excess total calories results in pathology similar to clinical NASH.

obesity; oxidative stress; tumor necrosis factor-alpha, CD36; liver fatty acid binding protein

NONALCOHOLIC FATTY LIVER DISEASE (NAFLD) is one of the most common liver pathologies and is closely associated with obesity and metabolic syndrome. NAFLD has been estimated to occur in 35% of lean and up to 70% of obese patients (83). As the incidence of obesity increased throughout the United States, there was a concomitant increase of NAFLD. There is a wide spectrum of NAFLD pathologies, ranging from simple reversible steatosis to nonalcoholic steatohepatitis (NASH) in which steatosis is accompanied by inflammation, necrosis, apoptosis, and fibrosis. Research into the molecular mechanisms underlying development of NASH pathology has been hampered by the lack of a suitable experimental animal model that mimics the natural course and etiological background of this disease in patients (19, 45). Three types of animal models have been pursued: *1*) Genetic models that result in obesity have been studied, such as models of hyperphagia [the JCR: LA-corpulent rat (24)]; models in which leptin or the leptin receptor are absent [ob/ob and db/db mice and fa/fa Zucker rats (7, 65)]; and models in which hepatic lipid metabolism is disrupted [peroxisome proliferator activator receptor α (PPARα) knockout mice (12)] or fatty acid synthesis is enhanced [sterol regulatory element binding protein-1c (SREBP-1c) transgenic mice (76)]. *2*) Pharmacological models using drugs to target hepatic triglyceride export by inhibiting apolipoprotein synthesis and assembly of very-low-density lipoprotein (43). *3*) Dietary deficiency models such as choline + methionine deficiency (18, 81). A common problem with all of these models is that they represent manipulations that do not reflect the natural etiological setting in which NAFLD/NASH develops clinically. More natural nutritional models in which animals have been fed diets high in sucrose, fructose, or fat ad libitum generally only result in obesity and hepatic steatosis without inflammation or necrosis (62, 77).

Recently, three new nutritional animal models for NASH have been described. In 2004, Lieber et al. (45) published a study in which male Sprague-Dawley rats were fed a high-fat liquid diet (71% energy from corn oil-olive oil-safflower oil) for 21 days; however, resulting hepatic pathology remained mild and no increase in serum alanine aminotransferase (ALT) activity occurred (45). This appears to be due to satiety limiting consumption of this high-fat diet ad libitum. In a second study, Deng et al. (19) utilized intragastric overfeeding of a 37% corn oil diet at 185% normal caloric intake over 9 wk to induce NASH pathology in male C57BL/6 mice. Development of obesity and insulin resistance was accompanied by liver hyperplasia, steatosis, inflammation, necrosis, and fibrosis. However, this model represents excessive overfeeding and some of the biochemical changes observed in the liver did not mimic those seen in NASH patients. For example, cytochrome *P*-450 2E1 (CYP2E1) expression was downregulated rather than upregulated and so was PPARα expression (19). Most recently, Wang et al. (80) compared feeding solid purified casein-based diets enriched with starch, sucrose, corn oil, or lard oil to male Wistar Crl(WI)BR rats for up to 24 wk. Sucrose, corn oil, and lard diets all resulted in steatosis; however, increased serum ALTs and apoptosis were observed in sucrose- and lard-fed rats, associated with evidence of endoplasmic reticulum stress,

Address for reprint requests and other correspondence: M. J. J. Ronis, Arkansas Children's Nutrition Center, Slot 512-20B, 1212 Marshall St., Little Rock, AR 72202 (e-mail: RonisMartinJ@uams.edu).

The costs of publication of this article were defrayed in part by the payment of page charges. The article must therefore be hereby marked "*advertisement*" in accordance with 18 U.S.C. Section 1734 solely to indicate this fact.

but did not occur in the corn oil-fed animals. Unlike the normal course of NASH in patients, severity of steatosis did not increase with time, liver damage developed rapidly prior to increases in body weight, and adiposity or TNF-α in these rats and was independent of changes in insulin signaling or mitochondrial function. Significant differences in molecular responses were observed between these dietary NASH models, and it is unclear whether these differences were related to species, rat strain, diet composition, or differences in experimental design or how reflective these models are of the human condition.

In the present study, we have examined the effects of moderate (17%) caloric excess and high dietary corn oil content on the development of NASH in male rats using a model in which overfeeding is accomplished by total enteral nutrition (TEN). This model is unique in that the TEN system represents a low-stress model in which the rats are essentially sedentary and NASH pathology very similar to that described clinically develops in response to feeding polyunsaturated fats (PUFA), despite homeostatic changes in fatty acid metabolism.

MATERIALS AND METHODS

Reagents. All chemicals were purchased from Sigma-Aldrich (St. Louis, MO) unless otherwise specified. Potassium chloride, potassium phosphate, and potassium ferricyanide were purchased from Fisher Scientific (Hampton, NH). ECL for chemiluminescent detection in Western blotting was purchased from Amersham Biosciences (Piscataway, NJ). TRI Reagent used for RNA extraction was obtained from Molecular Research Center (Cincinnati, OH). Reagents for assessment of RNA quality using the Agilent Bioanalyzer were acquired from Agilent Technologies (Foster City, CA).

Experimental animals and diets. Male Sprague-Dawley rats (175 g) were purchased from Harlan Sprague Dawley (Indianapolis, IN). Animals were housed in an Association for Assessment and Accreditation of Laboratory Animal Care approved animal facility. Animal maintenance and experimental treatments were conducted in accordance with ethical guidelines for animal research and were approved by the Institutional Animal Care and Use Committee at University of Arkansas for Medical Sciences. Rats had an intragastric cannula surgically inserted and were allowed 7 days to recover before diet infusion as described previously (2–5, 69). Animals had ad libitum access to water throughout the experiment.

Animals were randomly assigned to groups and infused diets containing 5% corn oil for 21 days at 187 kcal·kg$^{-3/4}$·day^{-1}, previously shown to maintain body weight gains equivalent to ad libitum chow-fed rats (2, 68) or were overfed isocaloric 220 kcal·kg$^{-3/4}$·day^{-1} diets (17% excess calories) containing 5, 10, 25, 35, 40, or 70% corn oil substituted for carbohydrate calories. Diet composition is given in Table 1. Protein, vitamin, and mineral content was the same in all diets (2). All diets met caloric and nutritional recommendations established by the National Research Council (NRC). One important aspect of this model is that the rats were essentially sedentary. Rats in metabolism cages have little opportunity for physical activity, except to eat and drink. When fed via TEN, the rats are even more sedentary because they do not need to work for food or water. We have documented this. Activity levels of rats were studied in metabolic cages equipped with a series of invisible light beams traversing each cage at difference distances from the cage floor. When a rat moved, one or more beams were broken and registered on a computer. The number of beam breaks per 24 h was used to calculate an activity that could be used to compare different treatment groups. Adult male Sprague-Dawley rats fed by TEN ($n = 6$) had 3,611.5 ± 186.3 units/24 h and rats having ad libitum access to standard commercially rodent foods and water ($n = 5$) had 6,285.4 ± 476.6 units/24 h ($P \leq 0.05$). In addition, the TEN system was designed to be very low stress. The animals were preconditioned to regular handling and housing in metabolic cages prior to cannulation and were also acclimated to the tether and to further handling after surgery and before the studies began. The unique headpiece design disperses the weight of the lightweight spring directly over the animal and permits the rat to assume all body positions for sleep, drinking, and 360° movement without any impairment of movement or pulling of the skin such as occurs with tether attached on the back or the neck. We have successfully utilized this system previously to study effects of chronic ethanol infusion on temporal sexually dimorphic patterns of growth hormone secretion, a parameter notoriously sensitive to stress (4).

Table 1. *Diet composition*

	5% Fat Diet[a,b]		70% Fat Diet[a,b]	
	Per Liter	Total kcal	Per Liter	Total kcal
Protein[c]	44 g	19%	44 g	19%
Carbohydrate[d]	169 g	76%	24.5 g	11%
Fat[e]	5.19 g	5%	72.7 g	70%

[a]The caloric density was 890 kcal/l and diets were fed at either 187 or 220 kcal/kg (75). [b]Vitamins and minerals added to meet or exceed National Research Council recommended levels. [c]Whey protein was supplemented with an amino acid mix to assure that all essential amino acids were present at levels to meet or exceed the National Research Council recommended levels. [d]25% Maltodextrin and 75% dextrose. [e]Corn oil (8.57 kcal/g).

Body weight gain was measured twice a week and at the beginning and end of the study. Total body fat composition was assessed by magnetic resonance imaging (Echo, Houston, TX). Rats were euthanized after 21 or 65 days of infusion, and serum and livers were collected and stored at −20 and −70°C, respectively.

Pathological evaluation. Liver pathology was assessed by hematoxylin-eosin and Oil Red O staining of liver sections and scored via blinded samples by a board-certified pathologist (L. Hennings). The pathology calculation was on the basis of ballooning degeneration (0–2), presence or absence of serum markers of necrosis (ALT score: cutoff was 55, based on data from Charles River Laboratories and our baseline values, $<55 = 0$, $>55 = 1$), the lipidosis score (based on MCID imaging analysis of Oil Red O-stained slides), and lobular inflammation/necrosis (0 = 0 foci, 1 = <2 foci, 2 = 2–4 foci, 3 = >4 foci). Apoptosis was assessed by in situ end labeling of free 3′-hydroxyl ends generated during apoptosis [terminal deoxynucleotidyl transferase-mediated dUTP nick-end labeling (TUNEL)] using a commercial kit (Frag-EL DNA Fragmentation Detection Kit, Fisher Scientific, Hampton, NH). The sections were counterstained with Gill's hematoxylin. Apoptotic bodies and cells appeared brown. At least 2,000 cells were counted from each liver section (5). Apoptosis was also assessed by immunohistochemical assessment of caspase 3 activation. Sections were pretreated with Dako EDTA antigen retrieval (pH 9.0) in a Dako tissue decloaker (Dako, Carpenteria, CA) according to manufacturer's directions for 20 min. Sections were then incubated in Dako Peroxidase block (Dako) for 10 min at room temperature, and rinsed three times in Tris-buffered salmet 0.1% Tween 20 (TBST). A 10% normal goat serum protein block (Vector Laboratories, Burlingame, CA) in TBST was applied for 30 min at room temperature. Sections were incubated in primary polyclonal antibody to cleaved caspase-3 (Asp175, Cell Signaling, Danvers, MA) at 1:00 dilution for 1 h at room temperature, rinsed three times with TBST, and incubated in secondary antibody [biotinylated goat anti-rabbit (Vector Laboratories)] at 1:400 dilution for 30 min at room temperature. Sections were rinsed three times with TBST, and the ABC reagent (Vector Laboratories) was applied for 30 min at room temperature. Sections were rinsed three times in TBST, and incubated in diaminobenzidine (Dako) for 3 min at room temperature, then rinsed in TBST, counterstained with Mayer's hematoxylin, and coverslipped. Slides were examined under a light microscope, and posi-

Table 2. *Primer sequences for real-time RT-PCR*

Gene Name	Forward Primer (5′-3′)	Reverse Primer (3′-5′)
Cyclophilin	GCATACAGGTCCTGGCATCT	TTCTTGCTGGTCTTGCCATT
TNF–α	ACTGAACTTCGGGGTGATTG	GCTTGGTGGTTTGCTACGAC
ADH1	CACCAAACCCATCCAGGAAGT	GCATGCTGAATGGCAGCTTAA
SREBP-1c	CAGAGGGACTACAGGCTGAGAAAG	CACGTAGATCTCTGCCAGTGTTG
ChREBP	GAAGACGGCGGAGTACATCCT	TGGCAGCATTGAGCTCCTCTA
FAS	TCGGCGAGTCTATGCCACTATT	CCGAGTAATGCCGTTCAGTTC
ACC	GCCCACTTTCTTCTATCACGCTAA	GAAGACGGCAGCATGAACTG
HADHA	CCCTCCACCCACGTACTAACC	TCGGTCTTTCTCCTGCTTCC
ACO	CACCTTCAATCCGGAGTTGATC	ATGCCATATTCCCTCATCTTCTTC
CPT-1	TCAACCTCGGACCCAAATTG	GCCCCGCAGGTAGATATATTCTT
L-FABP	ACCTCATCCAGAAAGGGAAGGA	GTGGATCACCTTGGACCCATAG
PDK4	GAAGATGCCTTTGAGTGTGCAA	GGTTGGCCTGGAAATTTTCC
HMGCS1	GCTTTGGTAGTTGCAGGAGACA	AGGAGCATTTGGCCCAATTAG
CYP2B2	TGTTTGGAGAGCGCTTTGACTA	CACCTGGCTGGAGAATGAACTT
SQLE	GGCAGAGCCCAATGTAAAGTTT	CCCCAGTCTCCTTGTCCTTGTA
CYP51	ACCATGGTGGGCAAGACTTTC	ACCGTAGACCTCTTCCGCATT
SCD1	TGCCAGAGGGAATAGGGAAA	GCCATTAGATATGGCCACCTTT
DCI	TTTGGTGGATGAGGTGGTACCT	TTCGTCAGCTGCCGAGAAT
CD36	GGCTGTGTTTGGAGGCATTCT	CCCGTTTTCACCCAGTTTTTG
PKLR	GGCTGTCTGAGCAAGACCTTTT	TGCTAACACGTCACTGGCTTTC
MTE1	GAATTGGGCTGCTTGGGATT	CACGGAGCCATTGATGACAAC
APOA4	CAACGCACAGACCCAGGATAT	CCATGGAGGACTGCAGGTTT
DUSP1	CTGGTAGTGACCCTCAAAGTGGTT	CTTACCATGCTTCCCGGAAAG
PRLR	GTGTGGATCATTGTGGCCATTC	GGTGGAAAGATGCAGGTCATCA
IDI1	GGATACCCTTGGAAGAGGTTGA	TCCGGATTCAGGGTTACATTCT

Gene-specific primers were designed by use of Primer Express Software (Applied Biosystems, Foster City, CA).

tive cells were counted in 10 randomly chosen ×200 fields. In rats infused with TEN diets for 65 days, portal and lobular fibrosis was detected by picrosirius red staining of collagen (72). Collagen staining was quantified in five randomly chosen ×40 fields using MCID Imaging Software version 7.0 linked to an Olympus Bx50 microscope.

Biochemical analysis. Nonesterified fatty acids (NEFA) were measured using the NEFA C kit from Waco Chemicals (Richmond, VA). Serum triglycerides were measured with Triglyceride Reagent (IR141; Synermed, Westfield, IN). Triglyceride was extracted from whole liver homogenates with chloroform-methanol (2:1, vol/vol) and analyzed using Triglyceride Reagent (IR141; Synermed). Serum glucose levels were measured with Glucose Reagent (IR071-072; Synermed, Westfield, IN). Serum insulin and leptin levels were measured using ELISA kits from Linco Research (St. Charles, MO) according to manufacturer's protocols. Serum adiponectin levels were measured with an ELISA kit from B-Bridge International (Sunnyvale, CA) according to manufacturer's protocols. Serum ALT levels were measured at death by using the Infinity ALT liquid stable reagent (Thermo Electron, Waltham, MA) according to manufacturer's protocols. Liver microsomes were prepared by differential centrifugation and stored at −70°C until analysis. Protein concentrations of the microsomes were determined by the Bradford method using the Bio-Rad Protein Assay (Bio-Rad, Hercules, CA). Liver lipid peroxidation was assessed as a measure of oxidative stress as described by Ohkawa et al. (59). Western immunoblot analysis of apoprotein expression for CYP2E1 and CYP4A1 was conducted as previously described (67) except that cross-reactive proteins were detected by enhanced chemiluminescence using horseradish peroxidase-linked goat antibody to rabbit IgG or rabbit antibody to sheep IgG in the case of CYP4A1. CYP2E1 was a gift from the laboratory of Dr. Magnus Ingelman-Sundberg (Karolinska Institute, Stockholm, Sweden) (37). CYP4Al was detected by using a polyclonal sheep antibody to rat CYP4A1 (78), which was a gift from Dr. Gordon Gibson (University of Surrey, Guildford, UK). TNF-α protein was stained in liver tissue sections with anti-TNF-α antibody (Abcam, Cambridge, MA).

Real-time reverse transcription-polymerase chain reaction. Total RNA was extracted from livers by using TRI Reagent and cleaned with RNeasy mini columns (Qiagen, Valencia, CA). RNA quality was ascertained spectrophotometrically (ratio of A260 to A280) and also

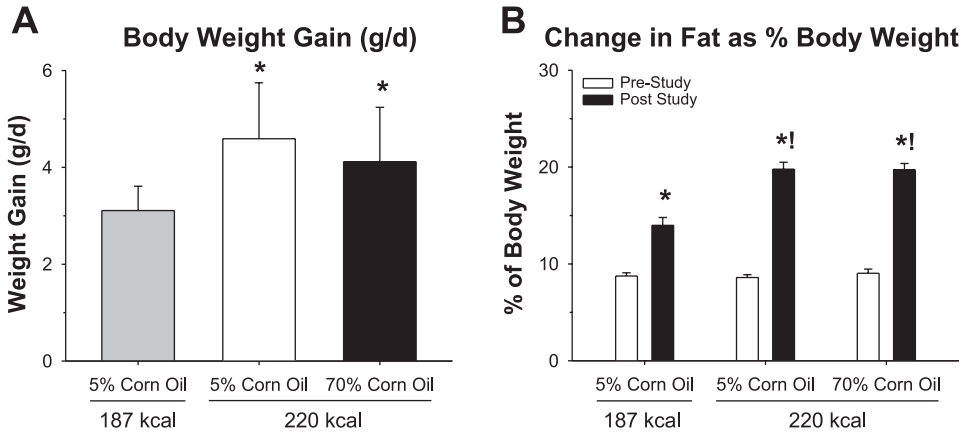

Fig. 1. Effects of overfeeding and high-fat intake on body weight and adiposity. *A*: body weight gain (g/day). Data represent means ± SE (n = 8–10). *$P \leq 0.05$ vs. 5% corn oil, 187 kcal·kg$^{-3/4}$·day^{-1}. *B*: change in fat mass as % body weight (pre- and poststudy). Data represent means ± SE (n = 8–10). *$P \leq 0.05$ prestudy vs. poststudy, !$P \leq 0.05$ vs. 5% corn oil, 187 kcal·kg$^{-3/4}$·day^{-1}.

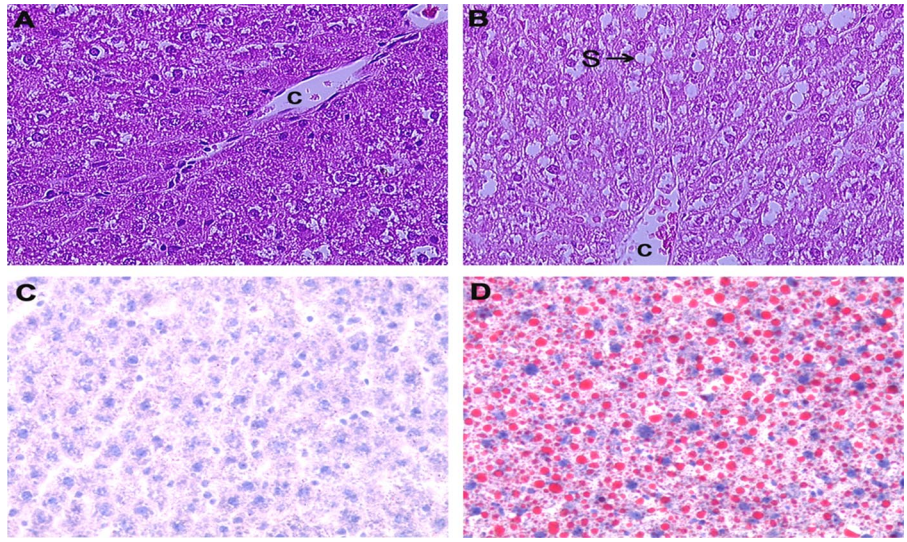

Fig. 2. Representative hematoxylin-eosin (H&E) and Oil Red O-stained liver sections. Representative H&E-stained liver sections of 5% corn oil, 220 kcal·kg$^{-3/4}$·day^{-1} (*A*) and 70% corn oil, 220 kcal·kg$^{-3/4}$·day^{-1} (*B*). Representative Oil Red O-stained liver sections of 5% corn oil, 220 kcal·kg$^{-3/4}$·day^{-1} (*C*) and 70% corn oil, 220 kcal·kg$^{-3/4}$·day^{-1} (*D*).

by checking the ratio of 28S to 18S ribosomal RNA using the RNA Nano Chip on a 2100 Bioanalyzer (Agilent Technologies, Palo Alto, CA). Total RNA (1 μg) was reverse transcribed by using the iScript Reverse Transcription kit (Bio-Rad Laboratories) according to manufacturer's instructions. The reverse transcribed cDNA (10 ng) was utilized for real-time PCR using the 2× SYBR green master mix and monitored on a ABI Prism 7000 sequence-detection system (Applied Biosystems, Foster City, CA). Gene-specific probes were designed by use of Primer Express Software (Applied Biosystems; Table 2), and the relative amounts of gene expression were quantitated by using a standard curve according to manufacturer's instructions.

Hepatic gene expression analysis. Hepatic gene expression profiles were assessed using Affymetrix RGU34A GeneChip microarrays (Affymetrix, Santa Clara, CA) containing 8,800 genes, with ~7,000 full-length transcripts and 1,800 EST sequences. Livers were excised from rats fed 5 or 70% corn oil diets (n = 3–4) containing 187 or 220 kcal·kg$^{-3/4}$·day^{-1}, respectively. Total RNA was extracted and prepared as described above. The intensity values of different probe sets (genes) generated by Affymetrix GeneChip Operating Software were imported into GeneSpring version 7.2 software (Silicon Genetics, Redwood City, CA) for data analysis. The data files (CEL files) containing the probe level intensities were processed by the robust multiarray analysis algorithm (GeneSpring) for background adjustment, normalization, and $\log_2$-transformation of perfect-match values (36). Subsequently, the data were subjected to per-chip and per-gene normalization by GeneSpring normalization algorithms. For comparison analysis, genes were filtered on the basis of minimum 1.5-fold ratio change and P value ≤0.05 using Student's t-test. Data analyses were performed using Microsoft Excel and GeneSpring GX v7.2. Correlation-based hierarchical clustering between treatment groups and visualization of data were done by using GeneSpring GX v7.2. Known biological functions of genes were queried and acquired from Affymetrix online data analysis resource NetAffx and gene ontology (GO) analyses performed using Affymetrix GO Browser (89). The original CEL files have been submitted to NCBI-GEO database and are accessible as series record GSE8253. Confirmation of microarray gene expression data was done by real-time RT-PCR.

EMSA. The nuclear extracts were isolated from livers frozen at −70°C using a nuclear extraction kit from Sigma. Protein concentration of the nuclear extracts was determined by the Bradford method using the Bio-Rad Protein Assay (Bio-Rad). Electrophoretic mobility shift assays (EMSAs) using double-stranded oligonucleotides coding for the acyl CoA oxidase (ACO)-peroxisome proliferator response element (PPRE), gatcCTCCCGAACGTGACCTTTGTC CTGGTCCAgatc, were performed as described previously (5, 87).

Statistical analysis. Data are expressed as means ± SE. Densitometric quantitation of Western blot autoradiograms was performed with Quantity One software (Bio-Rad). SigmaStat software package version 3.0 (SPSS, Chicago, IL) was used to perform all statistical tests. The data were tested with Levene's test for equality of variance. Pearson product moment correlation was performed with SigmaStat software. Group differences were evaluated via one- or two-way analysis of variance followed by Student-Newman-Keuls post hoc comparisons unless otherwise stated. P values ≤0.05 were considered statistically significant.

RESULTS

Effects of overfeeding and high-fat intake on body weight and adiposity. As in previous studies with the TEN model (2–5, 66, 68), infusion of diets at 187 kcal·kg$^{-3/4}$·day^{-1} resulted in weight gains similar to those in ad libitum chow-fed rats. Feeding a diet containing 220 kcal·kg$^{-3/4}$·day^{-1} represents a caloric intake of ~17% in excess of NRC recommended levels. Twenty-one days of overfeeding resulted in increases in final body weight from 281 ± 10 to 342 ± 3 g ($P \leq 0.05$). However, isocaloric increases in fat content from 5 to 70% at 220 kcal$^{3/4}$/day had no further effect on body weight (344 ± 11 g). The 2-fold increase in body weight gain in the 220 kcal$^{3/4}$/day groups ($P \leq 0.05$) (Fig. 1), was accom-

Table 3. *Hepatic pathology scores after 21-day TEN feeding*

	5% Corn Oil 220 kcal·kg$^{-3/4}$·day^{-1}	70% Corn Oil 220 kcal·kg$^{-3/4}$·day^{-1}
Serum marker of necrosis (ALTs)	0.0±0.0	1.0±0.0*
Hepatocellular ballooning	0.4±0.2	0.6±0.2
Lobular inflammation/necrosis	0.4±0.2	0.6±0.1
Lipidosis (Oil Red O staining)	1.8±0.6	2.6±0.8
Total score	2.6±0.6	4.8±0.4*

Values are mean ± SE; n = 8–10/group. TEN, total enteral nutrition. The pathology calculation was based on serum marker for necrosis [alanine aminotransferase (ALT) score: cutoff 55, based on data from Charles River Laboratories and our baseline values, <55 = 0, >55 = 1], ballooning degeneration (0–2), lobular inflammation/necrosis (0 = 0 foci, 1 = <2 foci, 2 = 2–4 foci and 3 = >4 foci), and the lipidosis score (base on evaluation of Oil Red O-stained slides). *$P \leq 0.05$ compared with 5% corn oil, 220 kcal·kg$^{-3/4}$·day^{-1}.

Table 4. *Biochemical effects of modest overfeeding of high-unsaturated fat diets*

Parameter	5% Corn Oil 220 kcal·kg$^{-3/4}$·day^{-1}	70% Corn Oil 220 kcal·kg$^{-3/4}$·day^{-1}
NEFAs, mmol/l	0.6±0.08	1.3±0.3*
Serum triglycerides, μg/μl	5.8±0.8	10.3±0.6*
Liver triglycerides, μg/g	5.5±0.5	8.9±1.6*
Serum insulin, ng/ml	1.6±0.3	3.1±0.5*
Adiponectin, μg/ml	10.6±1.6	4.5±0.9*
ALTs, U/l	19±1.9	70±4.0*
TUNEL, % apoptotic cells	0.1±0.02	0.4±0.05*
Caspase 3, % positive cells/×200 field	2.7±1.2	5.9±1.2
TBARS, nmol reactive TBA/mg protein	0.21±0.04	0.63±0.06*
TNF-α protein, proportional area	0.003±0.001	0.012±0.006*
TNF-α mRNA, relative expression	0.61±0.1	1.4±0.3*

Values are mean ± SE; n = 8–10/group. NEFAs, nonesterified fatty acids; TUNEL, terminal deoxynucleotidyltransferase-mediated dUTP nick-end labeling; TBARS, thiobarbituric acid (TBA)-reactive substances. *$P \leq 0.05$ compared with 5% corn oil, 220 kcal·kg$^{-3/4}$·day^{-1}.

panied by increased fat mass as % of body weight compared with those fed the 187 kcal·kg$^{-3/4}$·day^{-1} calorie diet ($P \leq 0.05$) (Fig. 1).

Effects of high-fat intake in the context of modest overfeeding on serum parameters. Increased caloric intake from 187 to 220 kcal·kg$^{-3/4}$·day^{-1} at 5% corn oil increased serum leptin (3.9 ± 0.4 to 7.2 ± 0.6 ng/ml) ($P \leq 0.05$) and serum glucose (92 ± 3.9 to 102 ± 5.8 mg/dl) ($P \leq 0.05$). Increasing dietary fat content isocalorically from 5 to 70% in the 220 kcal$^{3/4}$/day group resulted in no significant additional increases in serum leptin or glucose (leptin 8.9 ± 1.6 ng/ml, glucose 109 ± 3.8 mg/dl), but did significantly increase serum NEFAs and triglycerides ($P \leq 0.05$) (Table 4). In addition, serum insulin and adiponectin levels showed evidence of hyperinsulinemia and hypoadiponectinemia in the 70% corn oil, 220 kcal·kg$^{-3/4}$·day^{-1} group compared with the 5% corn oil, 220 kcal·kg$^{-3/4}$·day^{-1} group ($P \leq 0.05$) (Table 4).

Liver histopathology. Pathological examination demonstrated no histological evidence of fat accumulation or inflammation in the 187 kcal·kg$^{-3/4}$·day^{-1} (data not shown) or 220 kcal·kg$^{-3/4}$·day^{-1}, 5% corn oil groups (Fig. 2, Table 3), but steatosis, macrophage infiltration, and focal necrosis was present in the 220 kcal·kg$^{-3/4}$·day^{-1}, 70% corn oil group (Fig. 2, Table 3), accompanied by elevated serum ALT levels ($P \leq 0.05$) (Table 4) indicating necrotic injury. Increased levels of hepatocyte apoptosis were also present as determined by TUNEL analysis ($P \leq 0.05$) and a nonsignificant increase in activated caspase 3 expression (Table 4). Oil Red O staining and biochemical analysis of triglycerides showed a dose-dependent increase in triglyceride deposition with increase in percent of dietary corn oil (5 < 10 < 35 < 70%, only 5 and 70% shown) in 220 kcal·kg$^{-3/4}$·day^{-1} diets ($P \leq 0.05$) (Fig. 2, Table 3 and Table 4).

Effects of 65 days overfeeding of TEN diets high in PUFA. A more chronic study of 65 days, overfeeding of 220 kcal·kg$^{-3/4}$·day^{-1} high-corn oil TEN diets, demonstrated that development of NASH pathology and necrosis was not only dose responsive, but progressive with length of infusion. Feeding of diets containing 40% corn oil, 220 kcal·kg$^{-3/4}$·day^{-1} resulted in similar pathology to that observed with 70% corn oil, 220 kcal·kg$^{-3/4}$·day^{-1} for 3 wk (data not shown) and was accompanied by increased serum ALTs ($P \leq 0.05$) (Fig. 3). Histological examination of livers from the 65-day 70% corn oil-fed group revealed portal/periportal and lobular fibrosis as indicated by increased picrosirius red staining of collagen ($P \leq 0.05$) in addition to steatohepatitis, similar to that observed in grade 3 clinical NASH, accompanied by greater serum ALT values ($P \leq 0.05$) (Fig. 3).

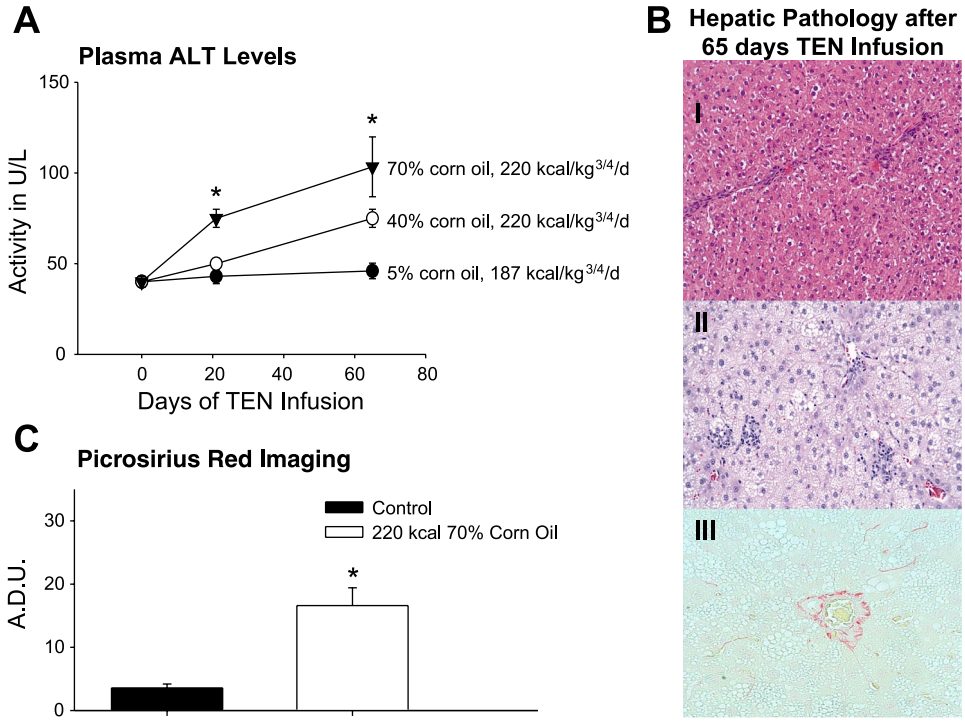

Fig. 3. Effects of 65-days total enteral nutrition (TEN) infusion. *A*: alanine aminotransferase activity levels over 65 days TEN infusion. Data represent means ± SE (n = 8–10). *$P \leq 0.05$ vs. 5% corn oil, 220 kcal·kg$^{-3/4}$·day^{-1}. *B*: representative liver sections of H&E-stained control liver (*I*); H&E stained liver after 65 days TEN infusion of 70% corn oil and 220 kcal·kg$^{-3/4}$·day^{-1} diet (*II*); and picrosirius red staining of portal and lobular collagen in liver after 65-days TEN infusion of 70% corn oil, 220 kcal·kg$^{-3/4}$·day^{-1} diet (*III*). *C*: quantitation of picrosirius red collagen staining by image analysis in control liver and after 65-day TEN infusion of 70% corn oil, 220 kcal·kg$^{-3/4}$·day^{-1} diet. A.D.U., arbitrary densitometric units.

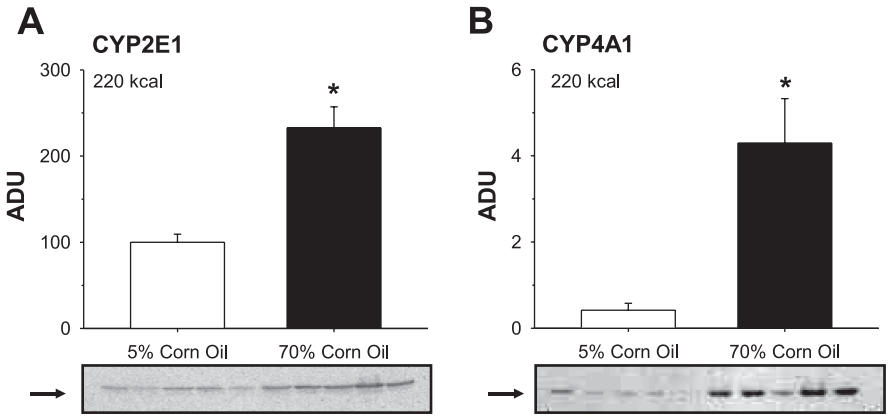

Fig. 4. Effects on hepatic CYP2E1 and CYP4A1 expression. *A*: densitometric quantitation of CYP2E1 protein levels from rats fed 5 or 70% corn oil, 220 kcal·kg$^{-3/4}$·day^{-1} and representative Western blot. Data represent means ± SE (n = 5). Each lane represents the liver microsomal protein from individual rats. *$P \leq 0.05$ vs. 5% corn oil, 220 kcal·kg$^{-3/4}$·day^{-1}. *B*: densitometric quantitation of CYP4A1 protein levels from rats fed 5 or 70% corn oil, 220 kcal·kg$^{-3/4}$·day^{-1} and representative Western blot. Data represent means ± SE (n = 5). Each lane represents the liver microsomal protein from individual rats. *$P \leq 0.05$ vs. 5% corn oil, 220 kcal·kg$^{-3/4}$·day^{-1}.

Effects of overfeeding high-fat diets on hepatic oxidative stress and inflammation. In the 70% corn oil, 220 kcal·kg$^{-3/4}$·day^{-1} group, an increase in oxidative stress [thiobarbituric acid-reactive substances (TBARSs); $P \leq 0.05$] and inflammation, as evidenced by TNF-α mRNA and protein induction ($P \leq 0.05$) was observed (Table 4). An increase in CYP2E1 and CYP4A1 expression ($P \leq 0.05$) (Fig. 4), sources of reactive oxygen species (ROS), was also observed.

Correlation between cell death, steatosis, oxidative stress, and inflammation. The correlations between ALTs (cell death) vs. Oil Red O staining (steatosis), TBARSs (oxidative stress) vs. steatosis, oxidative stress vs. cell death, and oxidative stress vs. TNF-α (inflammation) were significant ($P \leq 0.05$) (Table 5).

Fatty acid homeostasis. The appearance of steatosis in the TEN model after 21 days infusion was accompanied by significant decreases in mRNA expression for the rate limiting enzymes in de novo fatty acid (FA) synthesis: FA synthase (FAS) and acetyl CoA carboxylase (ACC), in the 220 kcal·kg$^{-3/4}$·day^{-1}, 70% corn oil group relative to the 220 kcal·kg$^{-3/4}$·day^{-1}, 5% corn oil group ($P \leq 0.05$) (Table 6). In addition, we observed decreases in mRNA encoding SREBP-1c and carbohydrate response element binding protein (ChREBP) ($P \leq 0.05$) (Table 6). In contrast, we observed significant increases in mRNAs for alcohol dehydrogenase (ADH) class I and PPARα-regulated enzymes involved in ω-oxidation of FA: CYP4A1 (endoplasmic reticulum FA ω-oxidation), ACO (peroxisomal FA β-oxidation), and mitochondrial trifunctional protein, alpha subunit (mitochondrial FA β-oxidation) and FA mitochondrial transport: carnitine palmitoyl transferase (Table 6). EMSA showed an increase in PPARα binding to its ACO-PPRE in the 70% corn oil group ($P \leq 0.05$) (Fig. 5). Microarray analysis of livers from the 187 kcal·kg$^{-3/4}$·day^{-1} 5% corn oil diet compared with 220 kcal·kg$^{-3/4}$·day^{-1} 70% corn oil diets was conducted using Affymetrix GeneChip microarray system. Seventy-seven genes were altered in the 70% corn oil group, using a 1.5-fold cutoff (Fig. 6). Many of these were genes involving fatty acid metabolism and transport. Steroyl CoA desaturase, known to be involved in regulation of fatty acid synthesis was downregulated 25-fold whereas mitochondrial acyl CoA thioesterase (MTE1), an enzyme involved in fatty acid β oxidation was upregulated 10-fold. This is consistent with homeostatic effects of steatosis on fatty acid synthesis and degradation (Table 7). A major gene to be upregulated fivefold was the scavenger receptor and known fatty acid transporter, CD36. We confirmed the regulation of these mRNAs using real-time PCR (Table 7). In addition, a second gene known to be involved in regulation of fatty acid transport, liver fatty acid binding protein (L-FABP), was upregulated in the 70% corn oil group ($P \leq 0.05$) (Table 6).

DISCUSSION

We have attempted to produce NASH pathology in the rat using modest overfeeding of a diet high in corn oil. The rats were housed in metabolic cages and enterally fed under low-stress, sedentary conditions. Overfeeding alone increased body weight, weight gain, and adiposity; however, no hepatic pathology, including little or no steatosis, was observed in either rat group fed 5% corn oil for 21 days despite the development of obesity, hyperleptinemia, and hyperglycemia in the overfed 220 kcal·kg$^{-3/4}$·day^{-1} group. In contrast, when dietary fat content was increased in the presence of overfeeding, a dose-dependent increase in macro- and microsteatosis, lobular inflammation, necrosis, and apoptosis was observed. In chronic 65-day studies we observed significant further increases in plasma ALT and the appearance of fibrosis, suggesting that the development of NASH pathology was also progressive with time.

A possible link between obesity and NASH is a role for disrupted adipokine signaling (11, 14, 33). Serum leptin levels were significantly increased in the present study in all the overfed groups. Leptin is recognized as a multifunctional protein (32), and it has been shown in rats that, even in the absence of the leptin signaling cascade, steatohepatitis and augmentation of oxidative stress could be observed; however, without leptin signaling, neither fibrosis nor hepatocellular carcinoma developed, suggesting that leptin plays a pivotal role in the progression of fibrosis and carcinogenesis in NASH

Table 5. *Correlation between characteristics of NASH observed in 70% corn oil groups*

	Correlation Coefficient
ALT activity vs. Oil Red O stain	$r^2 = 0.740$
TBARS activity vs. Oil Red O stain	$r^2 = 0.595$
TBARS activity vs. ALTs	$r^2 = 0.703$
TBARS activity vs. TNF-α immunostain	$r^2 = 0.581$

NASH, nonalcoholic steatohepatitis. $P \leq 0.05$; n = 8–10 per group.

Table 6. *Effects of 21-day TEN feeding on fatty acid synthesis, degradation, and transport*

Relative Expression	5% Corn Oil 220 kcal·kg$^{-3/4}$·day^{-1}	70% Corn Oil 220 kcal·kg$^{-3/4}$·day^{-1}
ADH-1 mRNA	1.7±0.2	2.5±0.4*
SREBP-1c mRNA	1.4±0.2	0.5±0.1*
ChREBP mRNA	0.5±0.04	0.3±0.1*
FAS mRNA	2.8±0.4	1.0±0.1*
ACC mRNA	4.0±0.5	1.3±0.3*
HADHA mRNA	0.9±0.1	1.4±0.1*
ACO mRNA	1.5±0.1	2.2±0.1*
CPT-1 mRNA	1.7±0.7	4.7±0.5*
L-FABP mRNA	0.9±0.1	1.6±0.1*

Values are mean ± SE; n = 8–10/group. *$P \leq 0.05$ compared with 5% corn oil, 220 kcal·kg$^{-3/4}$·day^{-1}.

(40). Serum adiponectin was significantly reduced by overfeeding increasing percent PUFA in this model. Serum adiponectin has also been shown to be reduced in NASH patients correlating with the severity of pathology and independent of the development of insulin resistance (33, 53, 70). Recent studies have reported that insulin resistance is present in almost all patients with NAFLD (15) and that the presence of central obesity, type 2 diabetes, or the severity of insulin resistance are predictors of NASH independent of the severity of steatosis (83). This study showed increasing the percentage of corn oil in the 220 kcal·kg$^{-3/4}$·day^{-1} diets produced significant increases in serum insulin, reductions in hepatic SREBP-1c, and increases in hepatic ADH I expression all consistent with development of systemic and hepatic insulin resistance (31).

NASH pathology in patients is characterized by evidence of oxidative stress including the appearance of oxidized proteins, DNA, and lipids (1, 11, 15, 29, 75) and the magnitude of oxidative stress has been shown to correlate with disease severity (1, 75). It has been suggested that oxidative stress represents a "second hit" whereby simple reversible steatosis progresses to the more severe pathologies of NASH and fibrosis (16). We observed a significant increase in oxidative stress (TBARSs). Oxidative stress may result from a number of sources but has been particularly linked to mitochondria. There is increasing evidence of mitochondrial dysfunction in patients with NASH (6, 10, 61, 70) and the appearance of megamitochondria in hepatocytes is common in NASH patients (6, 54). Oxidative damage to mitochondria results in reduced ATP formation and permeabilization of the mitochondrial membrane (42, 48). This membrane permeability transition results in release of death mediators such as cytochrome *c*, which can stimulate both apoptosis and necrosis depending on ATP concentrations (48). Both apoptosis and necrosis were significantly increased in our model. In addition to being an important cellular target of oxidative stress, uncoupled mitochondrial respiration is a major source of ROS and we have evidence for increased mitochondrial fatty acid oxidation in the present model (42, 48). Peroxisomal β-oxidation of fatty acids can also generate ROS (54). The cytochrome *P*-450 enzymes CYP4A1 and CYP2E1 both catalyze "leaky" redox cycles, which can also produce ROS during fatty acid metabolism in the endoplasmic reticulum or even in the absence of substrate (22, 41, 64, 74). CYP2E1 induction has been shown to occur in NASH patients (8, 84, 85) and is significantly increased in our NASH model. In this regard our rat data differ from the mouse

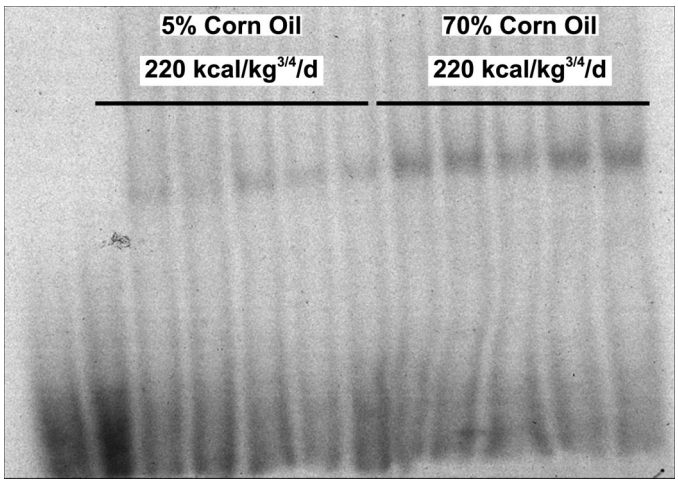

Fig. 5. EMSA analysis of PPARα binding to PPRE element of acyl CoA oxidase. *A*: representative EMSA showing the effect of rats fed 5 or 70% corn oil, 220 kcal·kg$^{-3/4}$·day^{-1} on hepatic PPARα binding to the PPRE in the ACO promoter. *Lanes 1–5* represent 5% corn oil, 220 kcal·kg$^{-3/4}$·day^{-1} and *lanes 6–10* represent 70% corn oil, 220 kcal·kg$^{-3/4}$·day^{-1}. Each lane is nuclear extract from an individual rat. Specificity of EMSA signal confirmed by competition with unlabeled and labeled oligonucleotides (not shown). Data represent means ± SE. Individual densitometry values of 5.8 ± 0.6 for 5% corn oil, 220 kcal·kg$^{-3/4}$·day^{-1} and 14.3 ± 1.4 for 70% corn oil, 220 kcal·kg$^{-3/4}$·day^{-1} are significantly different, $P \leq 0.05$.

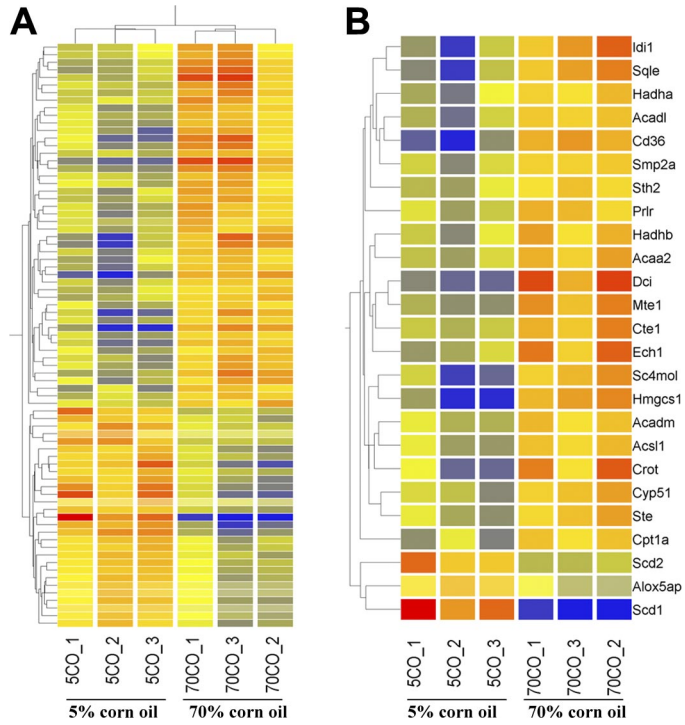

Fig. 6. Gene expression profiling of genes modulated by the NASH TEN model. *A*: heatmap representation of relative expression levels of genes modulated by 5% corn oil, 187 kcal·kg$^{-3/4}$·day^{-1} or 70% corn oil, 220 kcal·kg$^{-3/4}$·day^{-1} diet. Each horizontal line represents a single gene and each column represents a single sample. The relative expression of each gene is color coded as high (red) or low (blue); 77 genes are significant, $P \leq 0.05$ and 1.5-fold. *B*: heatmap clusters of gene expression of genes with biological, molecular, and cellular functions related to lipid metabolism; 25 genes were altered as classified by gene ontology.

Table 7. *Microarray analysis of the NASH TEN model*

Gene Identifier	Gene Description	Symbol	Microarray Ratio (NASH-70% corn oil/ Control-5% corn oil)	Real-Time RT-PCR (mRNA relative expression)	
		Acetyl-CoA biosynthesis and metabolism			
AF034577_at	Pyruvate dehydrogenase kinase 4	PDK4	**1.94**	1.2±0.2	1.5±0.3
rc_AI177004_s_at	3-Hydroxy-3-methylglutaryl-coenzyme A synthase 1	HMGCS1	**6.44**	2.7±0.5	6.4±0.9*
		Cell growth, cell adhesion, and cell-cell signaling			
M58634_at	Insulin-like growth factor binding protein 1	IGFBP1	0.32		
L21711_s_at	Lectin, galactose binding, soluble 5; lectin, galactose binding, soluble 9	LGALS5; LGALS9	0.61		
rc_AA893082_at	V-maf musculoaponeurotic fibrosarcoma (avian) oncogene homolog (c-maf)	MAF	0.61		
M74067_at	Claudin 3	CLDN3	0.63		
		Electron transport			
M13646_s_at	Cytochrome P450 3A11	CYP3A11	1.55		
M33312cds_s_at	Cytochrome P450 2A1 (hepatic steroid hydroxylase IIA1) gene	CYP2A1	1.62		
J02791_at	Acyl-CoA dehydrogenase, medium chain	ACADM	1.62		
M33936_s_at	Cytochrome P450 4A14	CYP4A14	1.67		
E01184cds_s_at	Cytochrome P450 1A2	CYP1A2	1.68		
X64401cds_s_at	Cytochrome P450 3A1; 3A3	CYP3A1; CYP3A3	1.71		
rc_AA997614_s_at	Cytochrome P450 51	CYP51	**1.92**	1.0±0.1	1.4±0.2
J05029_s_at	Acyl-CoA dehydrogenase, long-chain	ACADL	1.95		
U46118_at	Cytochrome P450 3A13	CYP3A13	2.29		
M13234cds_f_at	Cytochrome P450 2B polypeptide	CYP2B	**2.48**	0.8±0.02	1.2±0.2*
D37920_at	Squalene epoxidase	SQLE	**3.61**	1.6±0.4	4.0±0.8*
		Fatty acid biosynthesis, metabolism, and transport			
rc_AI175764_s_at	Stearoyl-coenzyme A desaturase 1	SCD1	**0.04**	2.8±0.5	0.1±0.1*
AF036761_g_at	Stearoyl-coenzyme A desaturase 2; similar to stearoyl-CoA desaturase 4	SCD2	0.47		
rc_AA800120_at	Solute carrier family 25 (carnitine/acylcarnitine translocase), member 20	SLC25A20	1.73		
D16478_g_at	Hydroxyacyl-coenzyme A dehydrogenase/3-ketoacyl-coenzyme A thiolase/enoyl-coenzyme A hydratase (trifunctional protein), alpha subunit	HADHA	1.75		
L07736_at	Carnitine palmitoyltransferase 1, liver	CPT1	1.85		
D16479_at	Hydroxyacyl-coenzyme A dehydrogenase/3-ketoacyl-coenzyme A thiolase/enoyl-coenzyme A hydratase (trifunctional protein), beta subunit	HADHB	1.86		
E12625cds_at	Sterol-C4-methyl oxidase-like	SC4MOL	3.26		
J02844_s_at	Carnitine *O*-octanoyltransferase	CROT	3.65		
rc_AA925752_at	CD36 antigen	CD36	**5.11**	0.4±0.1	2.1±0.3*
U08976_at	Enoyl coenzyme A hydratase 1	ECH1	2.93		
rc_AI170568_s_at	Dodecenoyl-coenzyme A delta isomerase	DCI	**5.85**	0.9±0.2	2.9±0.6*
		Fructose, glycogen metabolism, and glycolysis			
X05684_at	Pyruvate kinase, liver and RBC	PKLR	**0.24**	0.7±0.1	0.3±0.1*
rc_H31813_at	Similar to cDNA sequence BC021917 (predicted)	RGD1311026	0.37		
AF080468_g_at	Solute carrier family 37 (glycerol-6-phosphate transporter), member 4	SLC37A4	0.58		
rc_AA891785_g_at	Similar to NADP+-specific isocitrate dehydrogenase	LOC361596	0.63		
U10357_g_at	Pyruvate dehydrogenase kinase, isoenzyme 2	PDK2	0.65		
J04197_i_at	6-phosphofructo-2-kinase/fructose-2,6-biphosphatase 1	PFKFB1	0.65		
rc_AA891916_g_at	Membrane interacting protein of RGS16	MIR16	1.68		
		Lipid metabolism and transport			
M00002_at	Apolipoprotein A-IV	APOA4	**0.27**	0.5±0.1	0.2±0.1*
M33329_f_at	Rat senescence marker protein 2A gene, exons 1 and 2	SMP2A	1.62		
rc_AA893242_g_at	Acyl-CoA synthetase long-chain family member 1	ACSL1	1.78		
X05341_at	Acetyl-coenzyme A acyltransferase 2 (mitochondrial 3-oxoacyl-coenzyme A thiolase)	ACAA2	1.87		
Y09333_g_at	Mitochondrial acyl-CoA thioesterase 1	MTE1	**2.06**	1.1±0.2	5.0±1.7
		Protein and amino acid metabolism			
S81478_s_at	Dual specificity phosphatase 1	DUSP1	**0.5**	0.4±0.1	0.2±0.03*

Continued

Table 7.—*Continued*

Gene Identifier	Gene Description	Symbol	Microarray Ratio (NASH-70% corn oil/ Control-5% corn oil)	Real-Time RT-PCR (mRNA relative expression)	
D10756_at	Proteasome (prosome, macropain) subunit, alpha type 5	PSMA5	1.51		
D64045_s_at	Phosphatidylinositol 3-kinase, regulatory subunit, polypeptide 1	PIK3R1	1.63		
U13895_s_at	Proteasome (prosome, macropain) 26S subunit, ATPase 2	PSMC2	1.68		
rc_AI236795_s_at	Heat shock 90 kDa protein 1, beta	RGD1303075	1.69		
	Steroid biosynthesis				
M31363mRNA_f_at	Sulfotransferase 2A	STH2	1.53		
L48060_s_at	Prolactin receptor	PRLR	**1.72**	1.9±0.1	12.0±1.8*
S76489_s_at	Estrogen sulfotransferase	STE; STE2	1.91		
AF003835_at	Isopentenyl-diphosphate delta isomerase 1	IDI1	**3.97**	2.1±0.4	6.0±0.5*
	Other and unknown function				
rc_AA893552_at	Serine (or cysteine) proteinase inhibitor, clade A (alpha-1 antiproteinase, antitrypsin), member 4	SERPINA4	0.5		
AF045464_s_at	Aldo-keto reductase family 7, member A3 (aflatoxin aldehyde reductase)	AKR7A3	0.56		
rc_AA800613_at	Zinc finger protein 36	ZFP36	0.58		
rc_H33472_at	Transcribed locus		0.6		
rc_AA891790_at	Similar to hypothetical protein D10Ertd641e		0.6		
rc_AA893330_at	Similar to KIAA1324 protein (predicted)	RGD1310209	0.6		
Y15054_at	Coronin 7	CORO7	0.6		
U16686_at	Defensin, alpha 5,	DEFA	0.63		
Z17223_at	Mesenchyme homeo box 2	MEOX2	0.63		
rc_AI104781_at	Arachidonate 5-lipoxygenase activating protein	ALOX5AP	0.65		
rc_AA893384_g_at	Interferon regulatory factor 3	IRF3	0.66		
rc_AA800750_f_at	hypothetical protein LOC498544	LOC498544	0.66		
rc_AA894259_at	similar to RIKEN cDNA 2010110M21 (predicted)	RGD1309691	0.66		
rc_AI231445_at	Transcribed locus, strongly similar to NP_446458.1 unr protein [Rattus norvegicus]		1.52		
rc_AA859981_at	Inositol (myo)-1(or 4)-monophosphatase 2	IMPA2	1.63		
AB010635_s_at	Carboxylesterase 2 (intestine, liver)	CES2	1.72		
M63991_at	Serine (or cysteine) peptidase inhibitor, clade A (alpha-1 antipeptidase, antitrypsin), member 7	SERPINA7	1.83		
D38056_at	Ephrin A1	EFNA1	1.88		
X52815cds_f_at	Actin, gamma	ACTG	2.01		
AJ224120_at	Peroxisomal biogenesis factor 11A	PEX11A	2.07		
D00569_at	2,4-dienoyl CoA reductase 1, mitochondrial	DECR1	2.42		
rc_AA998683_g_at	Heat shock 27 kDa protein 1	HSPB1	2.58		

Results in bold were confirmed by real-time RT-PCR as shown; $n = 4–6$ per group. *$P \leq 0.05$.

intragastric overfeeding model of NASH developed by Deng et al. (19) in which CYP2E1 was found to be suppressed and where fatty acid oxidation appears downregulated. This may in part reflect species differences in hepatic responses to insulin and glucose. For example, the hepatotoxicity of xenobiotics in diabetic rats and mice are exactly the opposite as a result of differences in PPARα-mediated compensatory repair under conditions of disrupted insulin signaling and hyperglycemia. The response in human liver appears more similar to that seen in the rat (82).

Other pathways for NASH progression have also been suggested with oxidative stress representing only an epiphenomenal consequence of cellular injury (54). Cytokines, in particular TNF-α, have received much attention in the progression of NAFLD to NASH and also in development of steatosis itself (25). TNF-α protein and mRNA were both significantly increased in this study (Table 4). TNF-α expression is increased in both plasma and liver in NASH patients (13, 33) and animal models (17, 19) and is capable of producing insulin resistance, apoptosis/necrosis, and stellate cell activation (11). However, the role of TNF-α remains controversial. Anti-TNF therapy reduces NAFLD in the mouse ob/ob mouse (44) and steatosis was abolished in TNFR1 (−/−) mice fed high-carbohydrate diets (27); however, TNFR1 −/− mice have recently been shown not to be protected against development of liver pathology either in the intragastric overfed mouse model (19) or in methionine/choline-deficient mouse NASH models (17).

Direct "lipotoxicity" of excess circulating NEFAs has also been proposed as a progressor of NASH (73). We observed a significant increase in serum NEFA. Free FAs (FFAs) can produce apoptosis in hepatocytes directly (26, 73) and can destabilize lysosomes resulting in nuclear factor-κB-dependent TNF-α synthesis (27). However, lipotoxicity has been linked to long-chain saturated FAs such as palmitate (26, 27, 73) whereas the present study demonstrates that NASH pathology can be produced as the result of feeding corn oil, which consists primarily of PUFA. In alcoholic liver disease models, which have very similar hepatic pathology to NASH, several studies have demonstrated increased pathology associated with feeding PUFA or ω-3 FAs in fish oil whereas long- and

short-chain saturated fat diets are protective (55, 56, 68, 87). Studies are in progress to assess the effects of dietary fat composition on development of NASH pathology in rat in the TEN model. It has been suggested that the link between obesity, insulin resistance, and NASH risk is explained by increased release of FFA from adipose tissue (15). Insulin resistance increases lipolysis of adipose tissue depots, increasing FFA in NASH patients (49, 70). FFA transport into the liver has been proposed to stimulate PPARα, resulting in increased FA ω- and β-oxidation pathways as is observed in the present study (15).

Some animal studies of NASH have suggested that fat accumulation is the result of increased de novo FA synthesis. Hepatic FA synthesis has been suggested to be under the regulation by two transcription factors: SREBP-1c, which is regulated by fat and insulin, and ChREBP, which is regulated by dietary carbohydrates (20, 21). Both transcription factors stimulate expression of the rate limiting lipogenic genes FAS and ACC (20, 21). ACC activity is also regulated posttranscriptionally (52). In the overfed intragastric mouse model of NASH and in the JCR-LA corpulent rat SREBP-1c, FAS and ACC expression is increased (19, 23). In contrast, we have observed downregulation of mRNAs for SREBP1c, ChREBP, FAS, and ACC. Recent studies have suggested that suppression of SREBP-1c and ChREBP signaling is a specific hepatocyte response to PUFA, which are the major components of the corn oil utilized in the present study (20, 21, 38). The downregulation of SREBP-1c may also be a consequence of reduced expression of SCD-1 in these livers since this enzyme has been implicated in regulation of SREBP-1c and FA synthesis as the result of its ability to regulate cell signaling through conversion of palmitate to oleate (58, 63). Little is known regarding expression of these enzymes, SREBP-1c, or ChREBP in livers from NASH patients.

Two major proteins involved in FA uptake are L-FABP (34, 47, 57, 81) and the scavenger receptor, CD36 (46). CD36 is normally expressed at low levels in liver (86). Knockout of NADPH-cytochrome *P*-450 reductase or feeding of high-fat diets have recently been reported to significantly induce hepatic CD36 expression in mice coincident with the development of steatosis (35, 86); however, little is known about hepatic uptake of FFAs in animal models of NASH or in NASH patients. We have observed significant increases in expression of both L-FABP and CD36. This suggests that increased FA uptake plays a major role in the increased steatosis observed in this NASH model.

In summary, NASH is the most rapidly increasing hepatic pathology in the U. S. population and yet molecular mechanisms underlying NASH and methods to protect against it remain incompletely understood. This results from the absence of an animal model which replicates the natural course and etiology of the disease in patients. We have developed a new model of NASH in which hepatic pathology including fibrosis develops in sedentary rats under low-stress conditions as the result of moderate overconsumption of a diet similar to that consumed by Americans. Obviously, enteral feeding of liquid diets is not completely analogous to the human NASH situation. However, the TEN system uniquely allows dissection of the pathological effects of excessive caloric intake from the effects of imbalances in the major macronutrients thought to be involved in NASH and other related disorders of overweight and/or obesity. Pathological, endocrine, and biochemical changes were similar to those observed in NASH patients clinically and develop under conditions of obesity known to increase NASH incidence. However, hepatic steatosis and NASH develop rapidly in obese rats fed via TEN when the percentage of unsaturated dietary fat is increased. The mechanism of steatosis in this model does not involve altered FA synthesis or degradation but rather may involve increased FA transport via CD36 and/or L-FABP, genes known to be regulated via the PPAR transcription factors (34, 35, 46, 47, 57, 81, 86). Several biochemical endpoints including CYP2E1 expression, FA homeostasis, and PPARα-signaling differed between the present study other rodent NASH models. This may reflect differences in species, strain, diet composition, and experimental design. NASH appears to be a multifactorial condition in which the same pathological end points can be achieved by different routes. However, as in other animal models and in clinical samples from NASH patients, the appearance of liver pathology correlated with disruption of adipokines, evidence of insulin resistance, increases in hepatic oxidative stress, and increases in hepatic TNF-α expression. The commonalities between different models suggest that these pathways are of fundamental importance underlying the development of liver pathology in NAFLD.

ACKNOWLEDGMENTS

We thank the following people for their technical assistance: Matt Ferguson, Jamie Badeaux, Tammy Dallari, James M. Robinette, and Michele Perry.

GRANTS

This research was supported, in part, by RO1 AA 12819 (M. J. J. Ronis), ACNC-USDA-ARS 6251-51000-005D and the National Institute of Environmental Health Sciences Graduate Student Training Grant (J. N. Baumgardner).

REFERENCES

1. **Albano E, Mottaran E, Vidali M, Reale E, Saksena S, Occhino G, Burt AD, Day CP.** Immune response towards lipid peroxidation products as a predictor of progression of non-alcoholic fatty liver disease to advanced fibrosis. *Gut* 54: 987–993, 2005.
2. **Badger TM, Crouch J, Irby D, Hakkak R, Shahare M.** Episodic excretion of ethanol during chronic intragastric ethanol infusion in the male rat: continuous vs. cyclic ethanol and nutrient infusions. *J Pharmacol Exp Ther* 264: 938–943, 1993.
3. **Badger TM, Ronis MJ, Ingelman-Sundberg M, Hakkak R.** Pulsatile blood alcohol and CYP2E1 induction during chronic alcohol infusions in rats. *Alcohol* 10: 453–457, 1993.
4. **Badger TM, Ronis MJ, Lumpkin CK, Valentine CR, Shahare M, Irby D, Huang J, Mercado C, Thomas P, Ingelman-Sundberg M, Crouch J.** Effects of chronic ethanol on growth hormone secretion and hepatic cytochrome P450 isozymes of the rat. *J Pharmacol Exp Ther* 264: 438–447, 1993.
5. **Baumgardner JN, Shankar K, Korourian S, Badger TM, Ronis MJ.** Undernutrition enhances alcohol-induced hepatocyte proliferation in the liver of rats fed via total enteral nutrition. *Am J Physiol Gastrointest Liver Physiol* 293: G355–G364, 2007.
6. **Caldwell SH, Oelsner DH, Iezzoni JC, Hespenheide EE, Battle EH, Driscoll CJ.** Cryptogenic cirrhosis: clinical characterization and risk factors for underlying disease. *Hepatology* 29: 664–669, 1999.
7. **Carmiel-Haggai M, Cederbaum AI, Nieto N.** A high-fat diet leads to the progression of non-alcoholic fatty liver disease in obese rats. *FASEB J* 19: 136–138, 2005.
8. **Chalasani N, Gorski JC, Asghar MS, Asghar A, Foresman B, Hall SD, Crabb DW.** Hepatic cytochrome P450 2E1 activity in nondiabetic patients with nonalcoholic steatohepatitis. *Hepatology* 37: 544–550, 2003.
9. **Charlton M, Sreekumar R, Rasmussen D, Lindor K, Nair KS.** Apolipoprotein synthesis in nonalcoholic steatohepatitis. *Hepatology* 35: 898–904, 2002.

10. **Cortez-Pinto H, Chatham J, Chacko VP, Arnold C, Rashid A, Diehl AM.** Alterations in liver ATP homeostasis in human nonalcoholic steatohepatitis: a pilot study. *JAMA* 282: 1659–1664, 1999.
11. **Cortez-Pinto H, de Moura MC, Day CP.** Non-alcoholic steatohepatitis: from cell biology to clinical practice. *J Hepatol* 44: 197–208, 2006.
12. **Costet P, Legendre C, More J, Edgar A, Galtier P, Pineau T.** Peroxisome proliferator-activated receptor alpha-isoform deficiency leads to progressive dyslipidemia with sexually dimorphic obesity and steatosis. *J Biol Chem* 273: 29577–29585, 1998.
13. **Crespo J, Cayon A, Fernandez-Gil P, Hernandez-Guerra M, Mayorga M, Dominguez-Diez A, Fernandez-Escalante JC, Pons-Romero F.** Gene expression of tumor necrosis factor alpha and TNF-receptors, p55 and p75, in nonalcoholic steatohepatitis patients. *Hepatology* 34: 1158–1163, 2001.
14. **Czaja MJ.** Liver injury in the setting of steatosis: crosstalk between adipokine and cytokine. *Hepatology* 40: 19–22, 2004.
15. **Day CP.** Pathogenesis of steatohepatitis. *Best Pract Res Clin Gastroenterol* 16: 663–678, 2002.
16. **Day CP, James OF.** Steatohepatitis: a tale of two "hits"? *Gastroenterology* 114: 842–845, 1998.
17. **Dela Pena A, Leclercq I, Field J, George J, Jones B, Farrell G.** NF-kappaB activation, rather than TNF, mediates hepatic inflammation in a murine dietary model of steatohepatitis. *Gastroenterology* 129: 1663–1674, 2005.
19. **Deng QG, She H, Cheng JH, French SW, Koop DR, Xiong S, Tsukamoto H.** Steatohepatitis induced by intragastric overfeeding in mice. *Hepatology* 42: 905–914, 2005.
20. **Dentin R, Denechaud PD, Benhamed F, Girard J, Postic C.** Hepatic gene regulation by glucose and polyunsaturated fatty acids: a role for ChREBP. *J Nutr* 136: 1145–1149, 2006.
21. **Dentin R, Girard J, Postic C.** Carbohydrate responsive element binding protein (ChREBP) and sterol regulatory element binding protein-1c (SREBP-1c): two key regulators of glucose metabolism and lipid synthesis in liver. *Biochimie* 87: 81–86, 2005.
22. **Ekstrom G, von Bahr C, Ingelman-Sundberg M.** Human liver microsomal cytochrome P-450IIE1 Immunological evaluation of its contribution to microsomal ethanol oxidation, carbon tetrachloride reduction and NADPH oxidase activity. *Biochem Pharmacol* 38: 689–693, 1989.
23. **Elam MB, Wilcox HG, Cagen LM, Deng X, Raghow R, Kumar P, Heimberg M, Russell JC.** Increased hepatic VLDL secretion, lipogenesis, and SREBP-1 expression in the corpulent JCR:LA-cp rat. *J Lipid Res* 42: 2039–2048, 2001.
24. **Elam MB, Wilcox HG, Cagen LM, Deng X, Raghow R, Kumar P, Heimberg M, Russell JC.** Increased hepatic VLDL secretion, lipogenesis, and SREBP-1 expression in the corpulent JCR:LA-cp rat. *J Lipid Res* 42: 2039–2048, 2001.
25. **Endo M, Masaki T, Seike M, Yoshimatsu H.** TNF-alpha induces hepatic steatosis in mice by enhancing gene expression of sterol regulatory element binding protein-1c (SREBP-1c). *Exp Biol Med (Maywood)* 232: 614–621, 2007.
26. **Farrell GC, Larter CZ.** Nonalcoholic fatty liver disease: from steatosis to cirrhosis. *Hepatology* 43: S99–S112, 2006.
27. **Feldstein AE, Werneburg NW, Canbay A, Guicciardi ME, Bronk SF, Rydzewski R, Burgart LJ, Gores GJ.** Free fatty acids promote hepatic lipotoxicity by stimulating TNF-alpha expression via a lysosomal pathway. *Hepatology* 40: 185–194, 2004.
28. **Fisher EA, Ginsberg HN.** Complexity in the secretory pathway: the assembly and secretion of apolipoprotein B-containing lipoproteins. *J Biol Chem* 277: 17377–17380, 2002.
29. **Garcia-Monzon C, Martin-Perez E, Iacono OL, Fernandez-Bermejo M, Majano PL, Apolinario A, Larranaga E, Moreno-Otero R.** Characterization of pathogenic and prognostic factors of nonalcoholic steatohepatitis associated with obesity. *J Hepatol* 33: 716–724, 2000.
30. **Gusarova V, Brodsky JL, Fisher EA.** Apolipoprotein B100 exit from the endoplasmic reticulum (ER) is COPII-dependent, and its lipidation to very low density lipoprotein occurs post-ER. *J Biol Chem* 278: 48051–48058, 2003.
31. **He L, Simmen FA, Mehendale HM, Ronis MJ, Badger TM.** Chronic ethanol intake impairs insulin signaling in rats by disrupting Akt association with the cell membrane. Role of TRB3 in inhibition of Akt/protein kinase B activation. *J Biol Chem* 281: 11126–11134, 2006.
32. **Huang L, Li C.** Leptin: a multifunctional hormone. *Cell Res* 10: 81–92, 2000.
33. **Hui JM, Hodge A, Farrell GC, Kench JG, Kriketos A, George J.** Beyond insulin resistance in NASH: TNF-alpha or adiponectin? *Hepatology* 40: 46–54, 2004.
34. **Hung DY, Burczynski FJ, Chang P, Lewis A, Masci PP, Siebert GA, Anissimov YG, Roberts MS.** Fatty acid binding protein is a major determinant of hepatic pharmacokinetics of palmitate and its metabolites. *Am J Physiol Gastrointest Liver Physiol* 284: G423–G433, 2003.
35. **Inoue M, Ohtake T, Motomura W, Takahashi N, Hosoki Y, Miyoshi S, Suzuki Y, Saito H, Kohgo Y, Okumura T.** Increased expression of PPARgamma in high fat diet-induced liver steatosis in mice. *Biochem Biophys Res Commun* 336: 215–222, 2005.
36. **Irizarry RA, Hobbs B, Collin F, Beazer-Barclay YD, Antonellis KJ, Scherf U, Speed TP.** Exploration, normalization, and summaries of high density oligonucleotide array probe level data. *Biostatistics* 4: 249–264, 2003.
37. **Johansson I, Ingelman-Sundberg M.** Benzene metabolism by ethanol-, acetone-, and benzene-inducible cytochrome P-450 (IIE1) in rat and rabbit liver microsomes. *Cancer Res* 48: 5387–5390, 1988.
38. **Jump DB, Botolin D, Wang Y, Xu J, Christian B, Demeure O.** Fatty acid regulation of hepatic gene expression. *J Nutr* 135: 2503–2506, 2005.
39. **Kim S, Shin HJ, Kim SY, Kim JH, Lee YS, Kim DH, Lee MO.** Genistein enhances expression of genes involved in fatty acid catabolism through activation of PPARalpha. *Mol Cell Endocrinol* 220: 51–58, 2004.
40. **Kitade M, Yoshiji H, Kojima H, Ikenaka Y, Noguchi R, Kaji K, Yoshii J, Yanase K, Namisaki T, Asada K, Yamazaki M, Tsujimoto T, Akahane T, Uemura M, Fukui H.** Leptin-mediated neovascularization is a prerequisite for progression of nonalcoholic steatohepatitis in rats. *Hepatology* 44: 983–991, 2006.
41. **Leclercq IA, Farrell GC, Field J, Bell DR, Gonzalez FJ, Robertson GR.** CYP2E1 and CYP4A as microsomal catalysts of lipid peroxides in murine nonalcoholic steatohepatitis. *J Clin Invest* 105: 1067–1075, 2000.
42. **Lemasters JJ, Nieminen AL.** Mitochondrial oxygen radical formation during reductive and oxidative stress to intact hepatocytes. *Biosci Rep* 17: 281–291, 1997.
43. **Letteron P, Sutton A, Mansouri A, Fromenty B, Pessayre D.** Inhibition of microsomal triglyceride transfer protein: another mechanism for drug-induced steatosis in mice. *Hepatology* 38: 133–140, 2003.
44. **Li Z, Yang S, Lin H, Huang J, Watkins PA, Moser AB, Desimone C, Song XY, Diehl AM.** Probiotics and antibodies to TNF inhibit inflammatory activity and improve nonalcoholic fatty liver disease. *Hepatology* 37: 343–350, 2003.
45. **Lieber CS, Leo MA, Mak KM, Xu Y, Cao Q, Ren C, Ponomarenko A, DeCarli LM.** Model of nonalcoholic steatohepatitis. *Am J Clin Nutr* 79: 502–509, 2004.
46. **Luiken JJ, Willems J, Coort SL, Coumans WA, Bonen A, Van Der Vusse GJ, Glatz JF.** Effects of cAMP modulators on long-chain fatty-acid uptake and utilization by electrically stimulated rat cardiac myocytes. *Biochem J* 367: 881–887, 2002.
47. **Luxon BA, Milliano MT, Weisiger RA.** Induction of hepatic cytosolic fatty acid binding protein with clofibrate accelerates both membrane and cytoplasmic transport of palmitate. *Biochim Biophys Acta* 1487: 309–318, 2000.
48. **Malhi H, Gores GJ, Lemasters JJ.** Apoptosis and necrosis in the liver: a tale of two deaths? *Hepatology* 43: S31–S44, 2006.
49. **Marchesini G, Bianchi G.** Nutritional support with amino acids in advanced cirrhosis: a few answers, a lot of questions. *Nutrition* 15: 799–800, 1999.
50. **Mehta K, Van Thiel DH, Shah N, Mobarhan S.** Nonalcoholic fatty liver disease: pathogenesis and the role of antioxidants. *Nutr Rev* 60: 289–293, 2002.
51. **Miele L, Grieco A, Armuzzi A, Candelli M, Forgione A, Gasbarrini A, Gasbarrini G.** Hepatic mitochondrial beta-oxidation in patients with nonalcoholic steatohepatitis assessed by 13C-octanoate breath test. *Am J Gastroenterol* 98: 2335–2336, 2003.
52. **Munday MR, Milic MR, Takhar S, Holness MJ, Sugden MC.** The short-term regulation of hepatic acetyl-CoA carboxylase during starvation and re-feeding in the rat. *Biochem J* 280: 733–737, 1991.
53. **Musso G, Gambino R, De Michieli F, Cassader M, Rizzetto M, Durazzo M, Faga E, Silli B, Pagano G.** Dietary habits and their relations to insulin resistance and postprandial lipemia in nonalcoholic steatohepatitis. *Hepatology* 37: 909–916, 2003.
54. **Neuschwander-Tetri BA, Caldwell SH.** Nonalcoholic steatohepatitis: summary of an AASLD Single Topic Conference. *Hepatology* 37: 1202–1219, 2003.

55. **Nanjii AA.** Role of different dietary fatty acids in the pathogenesis of experimental alcoholic liver disease. *Alcohol* 34, 21–25, 2004.
56. **Nanjii AA, Jokelainen K, Tipoe GL, Rahemtulia A, Dannenberg AJ.** Dietary saturated fatty acids reverse inflammatory and fibrotic changes in the rat liver despite continued ethanol administration. *J Pharmacol Exp Ther* 299: 638–644, 2001.
57. **Newberry EP, Xie Y, Kennedy S, Han X, Buhman KK, Luo J, Gross RW, Davidson NO.** Decreased hepatic triglyceride accumulation and altered fatty acid uptake in mice with deletion of the liver fatty acid-binding protein gene. *J Biol Chem* 278: 51664–51672, 2003.
58. **Ntambi JM, Miyazaki M.** Regulation of stearoyl-CoA desaturases and role in metabolism. *Prog Lipid Res* 43: 91–104, 2004.
59. **Ohkawa H, Ohishi N, Yagi K.** Assay for lipid peroxides in animal tissues by thiobarbituric acid reaction. *Anal Biochem* 95: 351–358, 1979.
60. **Pan M, Cederbaum AI, Zhang YL, Ginsberg HN, Williams KJ, Fisher EA.** Lipid peroxidation and oxidant stress regulate hepatic apolipoprotein B degradation and VLDL production. *J Clin Invest* 113: 1277–1287, 2004.
61. **Perez-Carreras M, Del Hoyo P, Martin MA, Rubio JC, Martin A, Castellano G, Colina F, Arenas J, Solis-Herruzo JA.** Defective hepatic mitochondrial respiratory chain in patients with nonalcoholic steatohepatitis. *Hepatology* 38: 999–1007, 2003.
62. **Poulsom R.** Morphological changes of organs after sucrose or fructose feeding. *Prog Biochem Pharmacol* 21: 104–134, 1986.
63. **Rizki G, Arnaboldi L, Gabrielli B, Yan J, Lee GS, Ng RK, Turner SM, Badger TM, Pitas RE, Maher JJ.** Mice fed a lipogenic methionine-choline-deficient diet develop hypermetabolism coincident with hepatic suppression of SCD-1. *J Lipid Res* 47: 2280–2290, 2006.
64. **Robertson G, Leclercq I, Farrell GC.** Nonalcoholic steatosis and steatohepatitis. II. Cytochrome P-450 enzymes and oxidative stress. *Am J Physiol Gastrointest Liver Physiol* 281: G1135–G1139, 2001.
65. **Romics L Jr, Kodys K, Dolganiuc A, Graham L, Velayudham A, Mandrekar P, Szabo G.** Diverse regulation of NF-kappaB and peroxisome proliferator-activated receptors in murine nonalcoholic fatty liver. *Hepatology* 40: 376–385, 2004.
66. **Ronis MJ, Butura A, Sampey BP, Shankar K, Prior RL, Korourian S, Albano E, Ingelman-Sundberg M, Petersen DR, Badger TM.** Effects of N-acetylcysteine on ethanol-induced hepatotoxicity in rats fed via total enteral nutrition. *Free Radic Biol Med* 39: 619–630, 2005.
67. **Ronis MJ, Ingelman-Sundberg M, Badger TM.** Induction, suppression and inhibition of multiple hepatic cytochrome P450 isozymes in the male rat and bobwhite quail (Colinus virginianus) by ergosterol biosynthesis inhibiting fungicides (EBIFs). *Biochem Pharmacol* 48: 1953–1965, 1994.
68. **Ronis MJ, Korourian S, Zipperman M, Hakkak R, Badger TM.** Dietary saturated fat reduces alcoholic hepatotoxicity in rats by altering fatty acid metabolism and membrane composition. *J Nutr* 134: 904–912, 2004.
69. **Ronis MJ, Lumpkin CK, Ingelman-Sundberg M, Badger TM.** Effects of short-term ethanol and nutrition on the hepatic microsomal monooxygenase system in a model utilizing total enteral nutrition in the rat. *Alcohol Clin Exp Res* 15: 693–699, 1991.
70. **Sanyal AJ, Campbell-Sargent C, Mirshahi F, Rizzo WB, Contos MJ, Sterling RK, Luketic VA, Shiffman ML, Clore JN.** Nonalcoholic steatohepatitis: association of insulin resistance and mitochondrial abnormalities. *Gastroenterology* 120: 1183–1192, 2001.
71. **Sargin H, Sargin M, Gozu H, Orcun A, Baloglu G, Ozisik M, Seker M, Uygur-Bayramicli O.** Is adiponectin level a predictor of nonalcoholic fatty liver disease in nondiabetic male patients? *World J Gastroenterol* 11: 5874–5877, 2005.
72. **Saxena NK, Ikeda K, Rockey DC, Friedman SL, Anania FA.** Leptin in hepatic fibrosis: evidence for increased collagen production in stellate cells and lean littermates of ob/ob mice. *Hepatology* 35: 762–771, 2002.
73. **Schaffer JE.** Lipotoxicity: when tissues overeat. *Curr Opin Lipidol* 14: 281–287, 2003.
74. **Schattenberg JM, Wang Y, Singh R, Rigoli RM, Czaja MJ.** Hepatocyte CYP2E1 overexpression and steatohepatitis lead to impaired hepatic insulin signaling. *J Biol Chem* 280: 9887–9894, 2005.
75. **Seki S, Kitada T, Yamada T, Sakaguchi H, Nakatani K, Wakasa K.** In situ detection of lipid peroxidation and oxidative DNA damage in non-alcoholic fatty liver diseases. *J Hepatol* 37: 56–62, 2002.
76. **Shimano H, Horton JD, Hammer RE, Shimomura I, Brown MS, Goldstein JL.** Overproduction of cholesterol and fatty acids causes massive liver enlargement in transgenic mice expressing truncated SREBP-1a. *J Clin Invest* 98: 1575–1584, 1996.
77. **Surwit RS, Feinglos MN, Rodin J, Sutherland A, Petro AE, Opara EC, Kuhn CM, Rebuffe-Scrive M.** Differential effects of fat and sucrose on the development of obesity and diabetes in C57BL/6J and A/J mice. *Metabolism* 44: 645–651, 1995.
78. **Tamburini PP, Masson HA, Bains SK, Makowski RJ, Morris B, Gibson GG.** Multiple forms of hepatic cytochrome P-450. Purification, characterisation and comparison of a novel clofibrate-induced isozyme with other major forms of cytochrome P-450. *Eur J Biochem* 139: 235–246, 1984.
79. **Videla LA, Rodrigo R, Orellana M, Fernandez V, Tapia G, Quinones L, Varela N, Contreras J, Lazarte R, Csendes A, Rojas J, Maluenda F, Burdiles P, Diaz JC, Smok G, Thielemann L, Poniachik J.** Oxidative stress-related parameters in the liver of non-alcoholic fatty liver disease patients. *Clin Sci (Lond)* 106: 261–268, 2004.
80. **Wang D, Wei Y, Pagliassotti MJ.** Saturated fatty acids promote endoplasmic reticulum stress and liver injury in rats with hepatic steatosis. *Endocrinology* 147: 943–951, 2006.
81. **Wang G, Chen QM, Minuk GY, Gong Y, Burczynski FJ.** Enhanced expression of cytosolic fatty acid binding protein and fatty acid uptake during liver regeneration in rats. *Mol Cell Biochem* 262: 41–49, 2004.
82. **Wang T, Shankar K, Ronis MJJ, Mehendale HM.** Mechanisms and outcomes of drug- and toxicant-induced liver toxicity in diabetes. *Crit Rev Toxicol* 37: 413–439, 2007.
83. **Wanless IR, Lentz JS.** Fatty liver hepatitis (steatohepatitis) and obesity: an autopsy study with analysis of risk factors. *Hepatology* 12: 1106–1110, 1990.
84. **Weltman MD, Farrell GC, Hall P, Ingelman-Sundberg M, Liddle C.** Hepatic cytochrome P450 2E1 is increased in patients with nonalcoholic steatohepatitis. *Hepatology* 27: 128–133, 1998.
85. **Weltman MD, Farrell GC, Liddle C.** Increased hepatocyte CYP2E1 expression in a rat nutritional model of hepatic steatosis with inflammation. *Gastroenterology* 111: 1645–1653, 1996.
86. **Weng Y, DiRusso CC, Reilly AA, Black PN, Ding X.** Hepatic gene expression changes in mouse models with liver-specific deletion or global suppression of the NADPH-cytochrome P450 reductase gene. Mechanistic implications for the regulation of microsomal cytochrome P450 and the fatty liver phenotype. *J Biol Chem* 280: 31686–31698, 2005.
87. **You M, Considine RV, Leone TC, Kelly DP, Crabb DW.** Role of adiponectin in the protective action of dietary saturated fat against alcoholic fatty liver in mice. *Hepatology* 42: 568–577, 2005.
88. **Zammit VA.** Insulin stimulation of hepatic triacylglycerol secretion in the insulin-replete state: implications for the etiology of peripheral insulin resistance. *Ann NY Acad Sci* 967: 52–65, 2002.
89. **Zhang B, Schmoyer D, Kirov S, Snoddy J.** GOTree Machine (GOTM): a web-based platform for interpreting sets of interesting genes using Gene Ontology hierarchies (Abstract). *BMC Bioinformatics* 5: 16, 2004.